Sensorless Magnetic Model and PM Flux Identification of Synchronous Drives at Standstill

Sensorless Magnetic Model and PM Flux Identification of Synchronous Drives at Standstill

Paolo Pescetto, Gianmario Pellegrino
Politecnico di Torino, Energy department
Corso Duca degli Abruzzi 24, Torino, Italy
paolo.pescetto@polito.it

***Abstract*—This paper proposes a sensorless self-commissioning technique for PM-assisted synchronous reluctance motors. The identification of the machine's flux maps is performed at standstill without any position transducer and with no need of rotor locking. The machine is first excited with alternated high voltage pulses, injected in the estimated *d* and *q* directions of the rotor to determine its saturation curves. Then, direct current values are applied in a fixed stator direction so that the rotor aligns in specific positions giving information on the PM flux linkage. Experimental results are provided on a PM-assisted synchronous reluctance motor prototype, confirming the validity of the proposed method. The key original feature of the proposed work is the estimation of magnet flux linkage at standstill. For the motor under test, the magnet flux linkage was sensorless estimated at standstill with an error lower than 3%.**

Keywords*— *Sensorless, self-commissioning, PM drives, PM flux estimation, PM-Synchronous Reluctance Machines

I. Introduction

Recently, Synchronous Reluctance (SyR) motors became an attractive alternative to Induction Motors (IMs) and to Permanent Magnet Synchronous Machines (PMSMs) in a wide number of applications [1],[2]. The main advantages of SyR machines are their higher efficiency and better compactness when compared to IMs and their lower price when compared to PMSMs. Moreover, their inherently salient structure makes them highly suitable for sensorless operation, also at zero speed. However, pure SyR motors have a rather low power factor and non-ideal performance in the flux weakening speed range. Both these aspects can be considerably improved at low additional cost by the addition of small amount of permanent magnets (PM), obtaining a PM-assisted Synchronous Reluctance (PM-SyR) motor.

One key factor, limiting the adoption of both the SyR and the PM-SyR machines is their non-linear magnetic characteristics, showing direct and cross saturation between the two axes of the rotor. The knowledge of the flux maps of the machine has a relevant impact on the tuning of the drive control, and specific knowledge is required for both the machine commissioning and control tuning parts.

Dealing with the machine identification, the benchmark method for identification of the magnetic characteristic of synchronous motor drives is the constant speed technique in [3]. This method is very accurate, but requires a dedicated test rig and off-line identification of each new machine. In recent years, several self-commissioning techniques have been proposed [4]. Unfortunately, most of them require the presence of an encoder, locking the rotor or rotate the shaft at sufficiently high speed [5].

In [6], the authors propose to characterize the magnetic characteristic of PM synchronous motors by injecting a low amplitude square wave voltage with locked rotor and exploiting a position transducer. Recent works [7],[8] proposed a modification of this technique applied for SyR with high test voltages, compatible with the motor rated voltage. In this way, the flux maps identification is much less sensitive to inaccuracies in stator resistance estimation and to inverter nonlinear effects. Moreover, the identification has been performed in sensorless.

The magnet flux linkage λ_{pm} is usually evaluated by rotating the motor at constant speed at open circuit conditions, and measuring the back-electromotive force voltage [9]. Such operation requires a prime mover and voltage transducers, and it is necessarily performed off-line.

In this paper, the square wave injection self-identification technique of [8] is extended to PM-SyR motors. For the sake of brevity, the reported tests do not cover the cross-saturation current region. The results of the paper will be extended to such domain in future work. Specific problems related to the presence of permanent magnets are properly addressed. A solution for evaluating the PM flux linkage during the standstill identification session is proposed and tested. The obtained self-commissioning technique was experimentally validated on a 7 kW PM-SyR motor prototype.

II. Proposed the Self-Commissioning Method

The machine equations are briefly summarized. The voltage equations in rotor synchronous coordinates *dq* are:

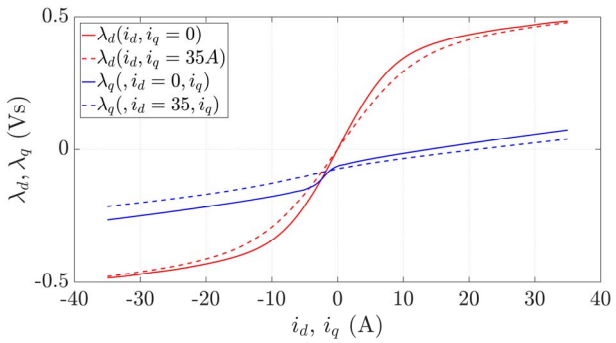

Fig. 1. Reference flux maps (2) measured at constant speed [3].

$$\begin{cases} v_d = R_s i_d + \frac{d\lambda_d}{dt} - \omega\lambda_q \\ v_q = R_s i_q + \frac{d\lambda_q}{dt} + \omega\lambda_d \end{cases} \quad (1)$$

Where λ_d, λ_q are the flux linkages in d and q axes, i_d, i_q the correspondent currents, R_s is the stator resistance and ω is the rotor speed in electrical [rad/s]. The relation between machine currents and fluxes is non-linear because of self-axis magnetic saturation and for the cross-coupling between d and q axes, as shown in Fig. 1.

$$\begin{cases} \lambda_d = \lambda_d(i_d, i_q) \\ \lambda_q = \lambda_q(i_d, i_q) \end{cases} \quad (2)$$

The motor torque T is calculated as:

$$T = \frac{3}{2} p(\lambda_d i_q - \lambda_q i_d) \quad (3)$$

Where p is the number of pole pairs.

A. PM Flux Component

The dq axes are aligned to the rotor following to the convention of synchronous reluctance machines, therefore the magnets point the negative q direction and the d axis indicates the direction of maximum inductance. The PM flux linkage λ_{pm} is hidden into the q axis flux component in (2) and is treated here as a negative offset of the flux linkage curves:

$$\lambda_q(i_d, i_q) = \lambda_{q0}(i_d, i_q) - \lambda_{pm} \quad (4)$$

Such approach is necessary since the proposed commissioning technique relies on AC excitation of the machine, which cannot capture the PM flux linkage component. In turn, the current dependent component of the q flux λ_{q0} will be identified through the AC test, whereas the PM flux linkage requires a dedicated set of test, newly proposed in this paper.

B. Flux Curves Identification

The saturation characteristic of the d and q directions are measured by extending the method proposed in [8] for SyR motors to the PM-SyR machine case. The motor is at standstill and free shaft, without using any position transducer. A square wave voltage of high amplitude is injected and the current response is acquired and processed to obtain the flux linkage curves. The excitation process is fast and produced torque is alternated at high frequency, so that the rotor can remain still during all the sequence with no need for mechanical locking.

Before the commissioning, the rotor position is evaluated using high frequency rotating signal injection techniques, such as [10], or parking the rotor through a dc current pulse. As said, it is assumed that the shaft will not move during the test, so that the estimated position of the d axis is used as a reasonable approximation of the real rotor position.

The test sequence is composed by two stages. At first, the estimated d axis is excited with a fast sequence of bipolar voltage pulses, while v_q is set to zero (***test #1***). The injected voltage is a square wave with an amplitude compatible with the rated motor voltage, as presented in [7],[8]. The voltage is controlled through a hysteresis mechanism, reversing its polarity when the current exceeds a maximum limit, as in Fig. 2.

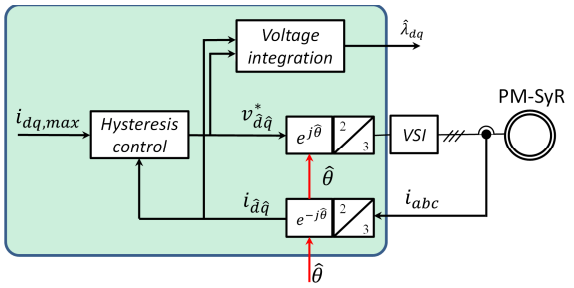

Fig. 2. Block diagram of drive controller used for *Test #1* and *Test #2*.

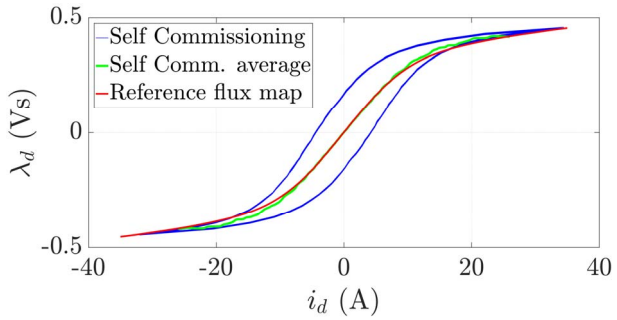

Fig. 3. Comparison between reference flux characteristic of $\lambda_d(i_d)$ (red), measured data in self commissionig (blue) and computed average curve (green).

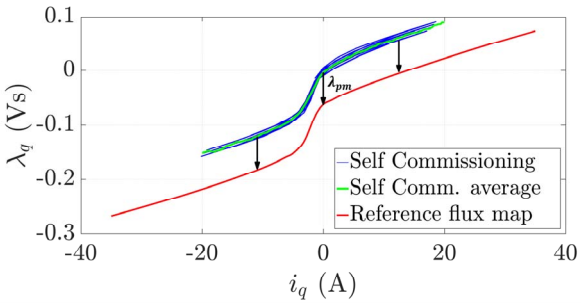

Fig. 4. Comparison between reference flux characteristic of $\lambda_q(i_q)$ (red), measured data in self commissioning for $\lambda_{q0}(i_q)$ (blue) and computed average curve (green). The term λ_{pm} is highlighted in black.

In this test, differently from [7],[8] torque is produced due to the presence of PM. Anyway, even if the shaft is free, the rotor does not move if the frequency of the injected voltage is high enough. This frequency is determined in the hysteresis control, depending on the voltage amplitude and desired current limits. Moreover, a high voltage amplitude improves the stability of the test, as demonstrated in [11]. The saturation characteristic of the d axis is evaluated through voltage integration:

$$\lambda_d(t) = \lambda_d(t = t_0) + \int_{t_0}^{t} (v_d - R_s i_d)\, dt \quad (5)$$

Then, the test is repeated on the q axis, whit v_d set to zero (***test #2***). The q axis saturation characteristic is estimated as:

$$\lambda_q(t) = \lambda_q(t = t_0) + \int_{t_0}^{t} (v_q - R_s i_q)\, dt \quad (6)$$

In this test, theoretically torque is not produced, so the rotor should not move. Anyway, the rotor is in an unstable equilibrium, since in case of inaccurate initial position detection the motor would produce a strong torque and the shaft starts to rotate. In this case, the test would fail. Detailed experimental solutions adopted to solve this problem are addressed in [11].

C. Data Manipulation

The output of the self-commissioning tests is in the form of hysteresis loops [11], as visible in Figs. 4 and 5. Moreover, the measured samples shown in blue in Fig. 3 and Fig. 4 are not regularly spaced in the current domain. Last, as open loop integrators are used, the flux estimates (5) and (6) tend to drift during the test, so the initial flux values $\lambda_d(t=t_0)$ and $\lambda_q(t=t_0)$ must be adjusted offline after the test. Altogether, the raw data coming from the identification require manipulation to get to the target flux characteristics $\lambda_d(i_d)$, $\lambda_q(i_q)$ in the form of regular look-up tables.

At first, the hysteresis loop is reorganized using the weighted average of the flux and current samples. For $\lambda_d(i_d)$ characteristic (test #1), the average curve is obtained as:

$$\lambda_{d,k} = \frac{\sum_{i=1}^{n_s} w_i \lambda_{dm,i}}{\sum_{i=1}^{n_s} w_i} \tag{7}$$

$$w_i = \frac{1}{(i_{dm,i} - i_{d,k})^4 + \frac{1}{w_{max}}} \tag{8}$$

Where n_s is the number of output samples of test #1, w_i is the weight of the i-th sample, i_{dm} is the vector of measured currents, λ_{dm} the vector of estimated fluxes obtained with (5), $\lambda_{d,k}$ and $i_{d,k}$ are elements of the desired look-up-table. The term w_{max} is introduced to limit the weights values avoiding singularities. The same procedure is adopted for test #2, obtaining the average curve of $\lambda_{q0}(i_q)$.

Alternatively, interpolating functions could be adopted, as in [7][8]. Such approach is intended of pure SyR machines and does not fit well with the presence of the PM flux linkage component.

Dealing with the control of the curves' drift, the d axis characteristic the problem can be easily fixed by applying (7) to an exact number of cycles and then imposing zero flux at zero i_d constraint:

$$\lambda_d(i_d = 0) = 0 \tag{9}$$

On the other hand, finding the correct offset for the q axis curve $\lambda_q(i_q)$ is much more challenging, and deals with the determination of the term λ_{pm}. For now, similarly to what done for the λ_d characteristic, it is imposed that the $\lambda_{q0}(i_q)$ curve is forced to zero at zero current.

$$\lambda_{q0}(i_q = 0) = 0 \tag{10}$$

The final curves forming the output look-up tables are represented in green in Fig. 3 and Fig. 4.

III. PM Flux Identification form Zero Torque Locus

A simple procedure to determine λ_{pm} at quasi-standstill is proposed. A dc current is injected through a PI mechanism in the stator alpha axis (rotor parking). The shaft will rotate until it reaches a stable position, where the torque is zero due to the balance between magnet and reluctance torque components. From manipulation of (3) and (4), the rest condition is found as:

$$T = \frac{3}{2} p(\lambda_d i_q - \lambda_{q0} i_d + \lambda_{pm} i_d) = 0 \tag{11}$$

This equation presents two possible solutions:

$$\begin{cases} i_d = 0 \\ \lambda_{pm} i_d = \lambda_{q0} i_d - \lambda_d i_q \end{cases} \tag{12}$$

The first solution ($i_d = 0$ and therefore $\lambda_d = 0$) is when the current vector is aligned with the magnets (q axis). The second solution is the when PM and reluctance effects are even (zero Nm contour in Fig. 5).

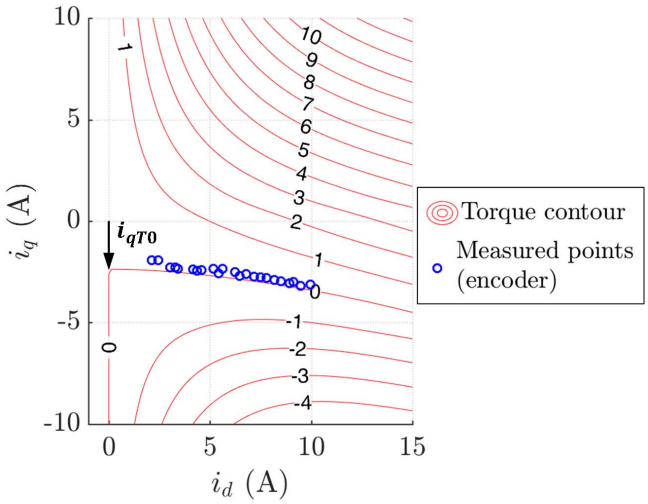

Fig. 5. Red lines: Torque contours in the dq current plane [Nm] for the motor under test. Blue dots: measured points using the encoder. The key value i_{qT0} is put in evidence.

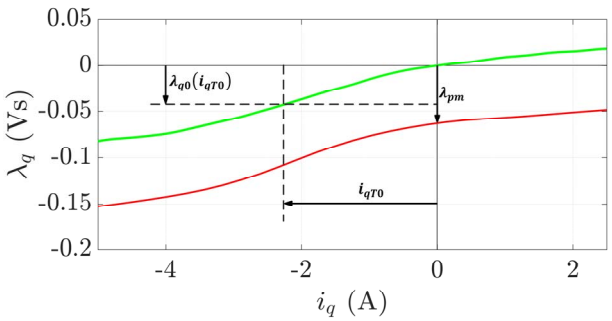

Fig. 6. Zoom of the reference $\lambda_q(i_q)$ (red) and the average of measured $\lambda_{q0}(i_q)$ (green). The terms λ_{pm}, $\lambda_{q0}(i_{qT0})$ and λ_{pm} are highlighted in black.

The magnet flux linkage λ_{pm} can be estimated using (12) and the saturation curves $\lambda_d(i_d), \lambda_{q0}(i_q)$ identified with the voltage excitation tests. This first approach would neglect the effect of cross saturation. Alternatively, the key current value i_{qT0} can be used to avoid the effect of cross-saturation, where i_{qT0} represents the value of i_q at the intercept between the zero Nm torque contour and the q axis, as indicated in Fig. 5. If equation (12) is applied to the singular point ($i_d = 0, i_{qT0}$), the PM flux can be estimated as:

$$\lambda_{pm} = \lambda_{q0}(i_{qT0}) - L_d i_{qT0} \tag{13}$$

Where $L_d = \lambda_d / i_d$ is evaluated in $i_d = 0$. The application of (13) is described in Fig. 6. This second approach is used in this work.

A. Evaluation of i_{qT0} with Current Excitation

The motor is controlled by a current loop in $\alpha\beta$ stationary reference frame, augmented by HF signal injection for sensorless position estimation (see Fig. 7). The HF injection algorithm will be explained in Section IV.

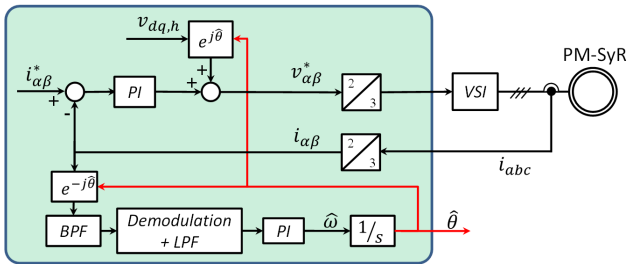

Fig. 7. Block scheme for the identification of PM flux linkage component.

The reference current vector is set in α axis ($i^*_\beta = 0$). Thanks to the free shaft condition, the rotor will move until the current vector lies on the zero torque locus, as shown in Fig. 8. In this condition, the rotor position θ is equal and opposite to the angle γ of the current vector in dq reference frame: $\gamma = -\theta$.

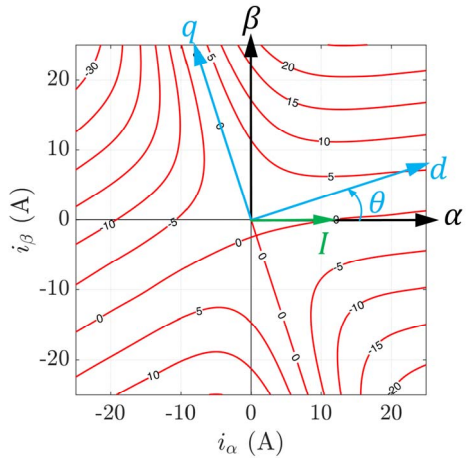

Fig. 8. Rotor alignment on the zero torque contour with DC current excitation along the α stator direction.

Therefore, from the current amplitude (imposed by the current loop) and rotor position (measured with encoder or sensorless estimated) it is possible to obtain a point on the zero Nm torque trajectory in the dq plane. Then, the test is repeated for different values of current amplitude, obtaining a set of points, represented in blue in Fig. 5.

Once measured enough points, i_{qT0} is determined by fitting the blue dots and extrapolating the trajectory to intercept the vertical axis. The zero torque locus is approximated with a bi-quadratic parabola having the maximum on the q axis:

$$i_q = -a i_q^4 + i_{qT0} \tag{14}$$

Where the parameters a and i_{qT0} can be easily found through Linear Least Square (LLS) procedure.

IV. Sensorless Determination of PM Flux Linkage

During the flux maps identification tests #1 and #2 the position is open loop evaluated only before the test, but real time position estimation can also be used to improve the test #2, as suggested in [12]. Sensorless position detection is necessary in the current excitation test used to determine i_{qT0} and therefore λ_{pm}. Two alternative strategies are proposed in this work.

A. Position Detection Technique

The self commissioning is performed at quasi standstill and there are not back-emf, therefore a saliency-based tracking loop is adopted. Such techniques are popular for sensorless control at standstill and differ one from the other mainly for the type of injected signal and for the demodulation algorithm. In this paper, similarly to [12], a pulsating HF square wave voltage at half of the switching frequency is injected in the estimated $\hat{d}$ axes while the HF current component in $\hat{q}$ axes is demodulated. In this way a position error signal is obtained and forced to zero through a position tracking loop. The adopted block scheme is represented in Fig. 7. This HF injection technique, proposed for the first time in [13], is chosen among the others in the literature because it is easy to tune, even with a limited knowledge of the flux maps. Details on the tracking loop tuning can be found in [12].

Neglecting the cross-coupling between d and q axes, the position error signal is:

$$i_{\hat{q}h} = \frac{u_c(L_d - L_q)}{4\omega_c L_d L_q}\sin(2\Delta\theta) \cong k_\varepsilon \cdot \Delta\theta \tag{15}$$

Where $i_{\hat{q}h}$ is the HF component of $i_{\hat{q}}$ after band-pass filter and demodulation process, u_c the injected voltage amplitude, L_d and L_q are differential inductances, ω_c the injection frequency and $\Delta\theta = \theta - \hat{\theta}$ is the position estimation error. Due to magnetic saturation, the inductances L_d, L_q and so the parameter k_ε are a function of the working point.

It must be noted that for high currents this position estimation technique will present error due to cross-saturation effect [14], especially for high anisotropy motors. The expected error due to cross-saturation effect $\Delta\theta_{cs}$ can be estimated as:

$$\Delta\theta_{dq}(i_d, i_q) = arctg\left(\frac{2l_{dq}}{l_d - l_q}\right) \tag{16}$$

Where l_d and l_q are the differential inductances in d and q axes and l_{dq} is the mutual inductance. Due to the differential inductance variability, also $\Delta\theta_{cs}$ is a function of the working point in the dq current plane. The literature proposes several methods to overcome this position error [14],[15], but the correction requires the knowledge of the flux maps, that is not available at this stage of the self commissioning procedure.

B. Continuous Current Excitation

As a first attempt, the current excitation test can be performed according to the block scheme in Fig. 7, setting increasing values of i^*_α while $i^*_\beta = 0$. In this way, the position is continuously observed when moving on the zero Nm torque trajectory in the fourth quadrant on the current plane.

As report in Fig. 9, the position estimation is good enough for low values of exciting current, but it's deteriorated for increasing i^*_α, resulting in a large discrepancy between the data

measured with the encoder (blue dots) and sensorless (black dots). This effect can be explained considering that in that area of the plane the cross-saturation error $\Delta\theta_{cs}$ becomes particularly relevant, as shown in Fig. 10, and therefore the correctness of the obtained i_{qT0} and λ_{pm} is compromised.

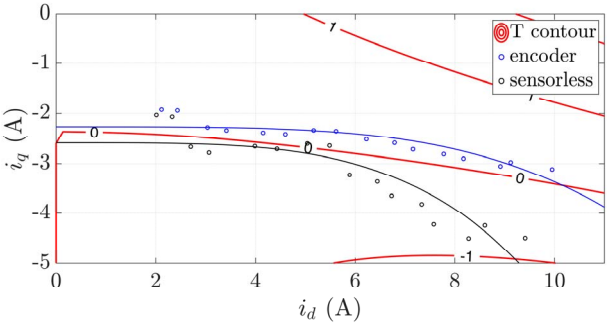

Fig. 9. Measured points on the zero Nm torque contour using the encoder (blue) or sensorless position tracking loop with continuous current excitation. The correspondent continuous lines are obtained via (14).

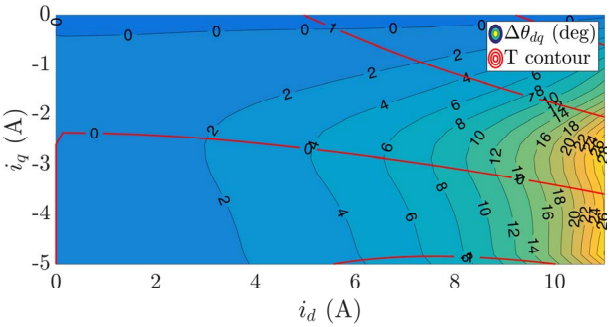

Fig. 10. Torque contour (red) and expected cross-saturation error $\Delta\theta_{cs}$ in the low torque area of dq current plane.

C. On-Off Current Excitation

To avoid such relatively high cross-saturation error, a feasible alternative is to iteratively switch on and off the current fundamental component, as shown in Fig. 11. The motor is excited with a dc current in α axis, aligning on the zero Nm torque contour as in Fig. 8. Then, the current is forced to zero, tacking care of not moving the rotor. Finally, the rotor position is sensorless estimated through HF signal injection. Assuming that the rotor position did not change when removing the dc current, a dot on the zero Nm trajectory is obtained. Then, the procedure is repeated for increasing current excitation.

The advantage of this technique is that the position is estimated when the current is in the origin of the dq plane, in a safe area with negligible cross-saturation error. Its main drawback is that transient torque may be produced when removing the dc current excitation, thus moving the rotor. Such eventual rotor movements would inevitably affect the position estimation and ultimately the evaluation of λ_{pm} and must be avoided. To prevent this effect it is suggested to excite the machine in stator $\alpha\beta$ coordinates, but switch to dq reference frame for de-excitation. In this way it is possible to regulate the d and q current components separately. If i_d is forced to zero prior to i_q, the current transient will pass in a safe area where the torque is very low. Therefore, the transient torque is reduced, preventing shaft movement.

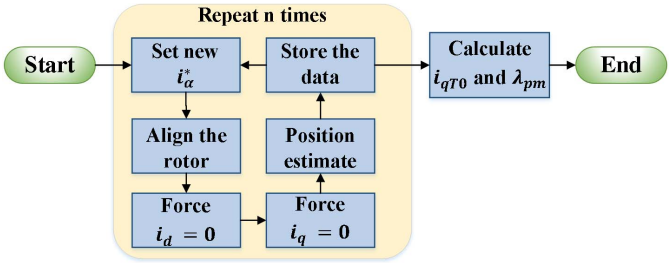

Fig. 11. Procedure for i_{qT0} and λ_{pm} evaluation with On-Off current excitation.

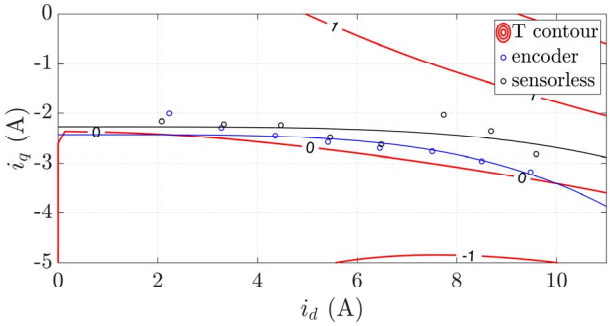

Fig. 12. Measured points on the zero Nm torque contour using the encoder (blue) or sensorless position tracking loop with On-Off current excitation. The correspondent continuous lines are obtained via (14).

V. Experimental Results

The proposed method was verified on a 7 kW PM-SyR motor prototype. The main characteristics of the machine under test are summarized in Table I.

TABLE I. Parameters of the Motor Under Test

Motor parameters	
Rated dc-link voltage (V)	360
Rated current (A)	28
Rated torque (Nm)	27
Rated speed (rpm)	2450
Pole pairs	2
Stator resistance (Ω)	0.9

A. Measurement of Flux Characteristic

At first, the reference flux maps of the motor where identified through the constant speed identification method of [3]. Then, the proposed standstill identification technique was implemented at free shaft, without locking the rotor and with the load disconnected. The obtained magnetization characteristics $\lambda_d(i_d)$ and $\lambda_{q0}(i_q)$ and their average curves extracted with (7) are shown in Fig. 3 and Fig. 4 (blue and green lines respectively). As can be seen, the flux curves obtained in self-commissioning are well in agreement with the reference characteristics, for both the axes. Dealing with λ_{q0} curve in Fig. 4, this is approximately at a constant distance from the reference curve λ_q. This confirms that the shift between the two curves is equal to λ_{pm}.

B. *Evaluation of λ_{pm}*

The DC current parking test described in section III was repeated for increasing values of current amplitude. The procedure was performed at first with continuous current excitation technique and then with the proposed On-Off excitation method. In each case, an encoder was used only for comparison purposes. The experimental results are report in Fig. 9 and Fig. 12. As can be seen, the samples obtained with continuous current excitation suffer for cross-saturation position error $\Delta\theta_{dq}$ for current amplitude higher than roughly 6 A. On the other hand, in the test performed with the On-Off excitation is immune from cross-coupling effects, but the shaft slightly moved from its equilibrium position during de-excitation for test currents higher than 8 A.

TABLE II. RESULTS: ESTIMATED MAGNET FLUX LINKAGE

	i_{qT0} (A)	λ_{pm} (Vs)	Relative error
Reference	-2.35	0.0620	-
Continuous excitation	-2.59	0.0644	-3.85 %
On-Off	-2.27	0.0563	9.13 %
Continuous + On-Off	-2.57	0.0638	-2.92 %
Encoder	-2.43	0.0603	2.82 %

Once obtained enough points in the dq current plane, the value of i_{qT0} was extrapolated using (14) for each set of measured data. Moreover, a further value for i_{qT0} was obtained putting together all the data measured in sensorless with continuous and with On-Off excitation. Finally, the magnet flux λ_{pm} was estimated via (13). The results are presented in Table II. The relative discrepancy obtained in sensorless using all the measured data is lower than 3 % and very similar to the result obtained with the encoder, proving the good accuracy of the proposed method. The obtained flux characteristic $\lambda_q(i_q)$ is compared with the reference flux maps in Fig. 13.

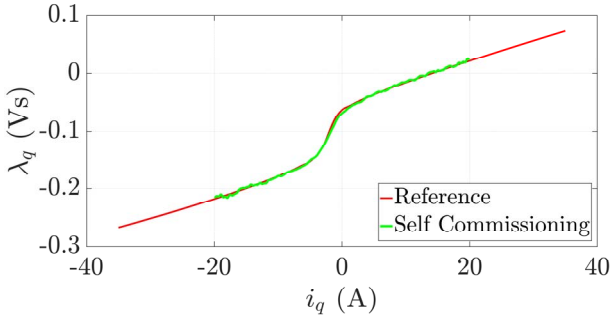

Fig. 13. Comparison between reference and measured characteristic $\lambda_q(i_q)$.

VI. CONCLUSIONS

The sensorless flux identification technique proposed in [8] for self-commissioning of SyR machines was successfully extended to PM-SyR motors. Specific issues due to the presence of PM were properly addressed. Moreover, the paper proposes an innovative method for the evaluation of the PM flux linkage component at quasi-standstill and free-shaft, which completes the flux maps identification. The technique exploits dc current excitation in stationary reference frame and sensorless HF signal injection position tracking loop. Experimental validation of the proposed method on a PM-SyR motor prototype proved its good accuracy with relative error lower than 3 %.

REFERENCES

[1] R. R. Moghaddam, "High speed operation of electrical machines, a review on technology, benefits and challenges," *2014 IEEE Energy Conversion Congress and Exposition (ECCE)*, Pittsburgh, PA, 2014, pp. 5539-5546.

[2] IEEE Guide for Test Procedures for Synchronous Machines Part IAcceptance and Performance Testing Part IITest Procedures and Parameter Determination for Dynamic Analysis - Redline," in IEEE Std 115-2009 (Revision of IEEE Std 115-1995) - Redline , vol., no., pp.1-219, May 7 2010.

[3] E. Armando, R. I. Bojoi, P. Guglielmi, G. Pellegrino and M. Pastorelli, "Experimental Identification of the Magnetic Model of Synchronous Machines," in *IEEE Transactions on Industry Applications*, vol. 49, no. 5, pp. 2116-2125, Sept.-Oct. 2013.

[4] S. A. Odhano, R. Bojoi, M. Popescu and A. Tenconi, "Parameter identification and self-commissioning of AC permanent magnet machines - A review," *2015 IEEE Workshop on Electrical Machines Design, Control and Diagnosis (WEMDCD)*, Torino, 2015, pp. 195-203.

[5] H. P. Nee, L. Lefevre, P. Thelin and J. Soulard, "Determination of d and q reactances of permanent-magnet synchronous motors without measurements of the rotor position," in *IEEE Transactions on Industry Applications*, vol. 36, no. 5, pp. 1330-1335, Sep/Oct 2000.

[6] G. Stumberger, T. Marcic, B. Stumberger and D. Dolinar, "Experimental Method for Determining Magnetically Nonlinear Characteristics of Electric Machines With Magnetically Nonlinear and Anisotropic Iron Core, Damping Windings, and Permanent Magnets," in *IEEE Transactions on Magnetics*, vol. 44, no. 11, pp. 4341-4344, Nov. 2008.

[7] N. Bedetti, S. Calligaro and R. Petrella, "Stand-Still Self-Identification of Flux Characteristics for Synchronous Reluctance Machines Using Novel Saturation Approximating Function and Multiple Linear Regression," in *IEEE Transactions on Industry Applications*, vol. 52, no. 4, pp. 3083-3092, July-Aug. 2016.

[8] M. Hinkkanen; P. Pescetto; E. Molsa; S. E. Saarakkala; G. Pellegrino; R. Bojoi, "Sensorless self-commissioning of synchronous reluctance motors at standstill without rotor locking," in IEEE Transactions on Industry Applications , vol.PP, no.99, pp.1-1

[9] A. Cavagnino, M. Lazzari, F. Profumo and A. Tenconi, "Axial flux interior PM synchronous motor: parameters identification and steady-state performance measurements," in *IEEE Transactions on Industry Applications*, vol. 36, no. 6, pp. 1581-1588, Nov/Dec 2000.

[10] M. Boussak, "Implementation and experimental investigation of sensorless speed control with initial rotor position estimation for interior permanent magnet synchronous motor drive," in IEEE Transactions on Power Electronics, vol. 20, no. 6, pp. 1413-1422, Nov. 2005.

[11] P. Pescetto and G. Pellegrino, "Sensorless Standstill Commissioning of Synchronous Reluctance Machines with Automatic Tuning," in proc. IEEE IEMDC 2017, Miami, Florida, May 2017.

[12] P. Pescetto and G. Pellegrino, "Sensorless Commissioning of Synchronous Reluctance Machines Augmented with High Frequency Voltage Injection," *2017 IEEE Energy Conversion Congress and Exposition (ECCE)*, Cincinnaty, OH, 2017.

[13] Y. D. Yoon, S. K. Sul, S. Morimoto and K. Ide, "High-Bandwidth Sensorless Algorithm for AC Machines Based on Square-Wave-Type Voltage Injection," in IEEE Transactions on Industry Applications, vol. 47, no. 3, pp. 1361-1370, May-June 2011.

[14] A. Yousefi-Talouki, P. Pescetto and G. Pellegrino, "Sensorless Direct Flux Vector Control of Synchronous Reluctance Motors Including Standstill, MTPA, and Flux Weakening," in *IEEE Transactions on Industry Applications*, vol. 53, no. 4, pp. 3598-3608, July-Aug. 2017.

[15] T. Tuovinen and M. Hinkkanen, "Adaptive Full-Order Observer With High-Frequency Signal Injection for Synchronous Reluctance Motor Drives," in *IEEE Journal of Emerging and Selected Topics in Power Electronics*, vol. 2, no. 2, pp. 181-189, June 2014.